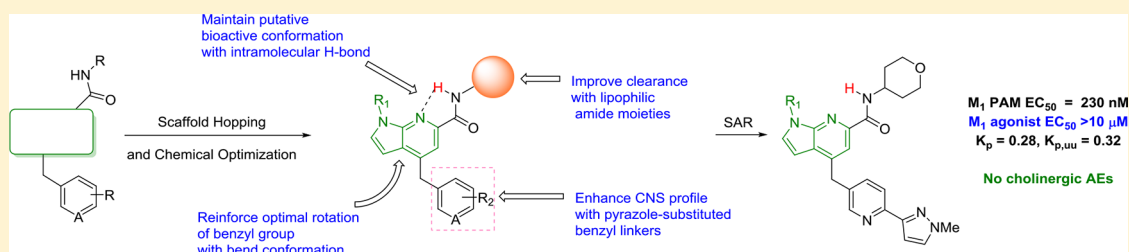


VU6007477, a Novel M<sub>1</sub> PAM Based on a Pyrrolo[2,3-*b*]pyridine Carboxamide Core Devoid of Cholinergic Adverse EventsJulie L. Engers,<sup>†,‡</sup> Elizabeth S. Childress,<sup>†,‡</sup> Madeline F. Long,<sup>†,‡</sup> Rory A. Capstick,<sup>†,‡</sup> Vincent B. Luscombe,<sup>†,‡</sup> Hekyung P. Cho,<sup>†,‡</sup> Jonathan W. Dickerson,<sup>†,‡</sup> Jerri M. Rook,<sup>†,‡</sup> Anna L. Blobaum,<sup>†,‡</sup> Colleen M. Niswender,<sup>†,‡,⊥</sup> Darren W. Engers,<sup>†,‡</sup> P. Jeffrey Conn,<sup>†,‡,⊥</sup> and Craig W. Lindsley<sup>\*,†,‡,§,||</sup><sup>†</sup>Vanderbilt Center for Neuroscience Drug Discovery, <sup>‡</sup>Department of Pharmacology, <sup>§</sup>Department of Chemistry, <sup>||</sup>Department of Biochemistry, and <sup>⊥</sup>Vanderbilt Kennedy Center, School of Medicine, Vanderbilt University, Nashville, Tennessee 37232, United States

## Supporting Information



**ABSTRACT:** Herein, we report the chemical optimization of a new series of M<sub>1</sub> positive allosteric modulators (PAMs) based on a novel pyrrolo[2,3-*b*]pyridine core, developed via scaffold hopping and iterative parallel synthesis. The vast majority of analogs in this series proved to display robust cholinergic seizure activity. However, by removal of the secondary hydroxyl group, VU6007477 resulted with good rat M<sub>1</sub> PAM potency (EC<sub>50</sub> = 230 nM, 93% ACh max), minimal M<sub>1</sub> agonist activity (agonist EC<sub>50</sub> > 10 μM), good CNS penetration (rat brain/plasma K<sub>p</sub> = 0.28, K<sub>p,uu</sub> = 0.32; mouse K<sub>p</sub> = 0.16, K<sub>p,uu</sub> = 0.18), and no cholinergic adverse events (AEs, e.g., seizures). This work demonstrates that within a chemical series prone to robust M<sub>1</sub> ago-PAM activity, SAR can result, which affords pure M<sub>1</sub> PAMs, devoid of cholinergic toxicity/seizure liability.

**KEYWORDS:** Positive allosteric modulator (PAM), muscarinic acetylcholine receptor 1 (M<sub>1</sub>), cholinergic toxicity, VU6007477

Muscarinic acetylcholine receptor subtype 1 (M<sub>1</sub>) positive allosteric modulators (PAMs) hold great promise for the treatment of cognitive impairment, schizophrenia, and Alzheimer's disease.<sup>1–7</sup> Originally, the clinical promise of M<sub>1</sub> as a target was derailed by M<sub>1</sub> agonists lacking true M<sub>1</sub> selectivity,<sup>1,2,8</sup> and later, by robust M<sub>1</sub> ago-PAMs that overstimulated the M<sub>1</sub> receptor, resulting in cholinergic toxicity and adverse events (AEs).<sup>9–18</sup> While these ago-PAMs, represented by 1–4 (Figure 1), dampened enthusiasm for the translational utility of selective M<sub>1</sub> activation, next generation M<sub>1</sub> PAMs 5 and 6, devoid of agonism in cells and native systems (and without cholinergic toxicity/seizures), provided a new path to the clinic.<sup>14,19</sup> However, due to the voluminous literature with ago-PAMs 1–4, multiple new M<sub>1</sub> PAMs are required for the community to evaluate the safety and efficacy of the “pure” M<sub>1</sub> PAM mechanism and independently embrace the therapeutic potential of M<sub>1</sub> PAMs. Herein, a novel series of M<sub>1</sub> PAMs featuring a pyrrolo[2,3-*b*]pyridine carboxamide core is described, including the design, SAR, DMPK properties, pharmacology, and cholinergic adverse effect profiles to provide the community with another new, pure M<sub>1</sub> PAM tool for *in vivo* efficacy and tolerability studies.

Scaffold-hopping has been a major strategy in the M<sub>1</sub> PAM arena, and this approach led to the discovery of the benzomorpholine-based pure M<sub>1</sub> PAM 6.<sup>19</sup> We once again held the key carboxamide and heterobiaryl tail moieties of 3, 5, and 6 constant while surveying new heterobiaryl cores, as in 7, that might engender pure M<sub>1</sub> PAM pharmacology (Figure 2). From this exercise, a novel pyrrolo[2,3-*b*]pyridine carboxamide core, represented generically by 8, resulted, with a spectrum of M<sub>1</sub> pharmacology from potent ago-PAMs to pure PAMs.

The synthesis of diverse analogs 13 (Scheme 1) proved straightforward with readily available starting materials from commercial sources.<sup>20</sup> 4-Chloro-1*H*-pyrrolo[2,3-*b*]pyridine-6-carbonitrile 9 could be alkylated with various R<sub>1</sub> moieties, but we first explored methyl. Conversion to the boronate ester under standard conditions provided 10 in >90% yield for the two steps. Suzuki coupling with either benzyl halides or heteroaryl methyl halides 11 generated derivatives 12 in 50–84% yield. Finally,

Received: June 7, 2018

Accepted: September 4, 2018

Published: September 4, 2018

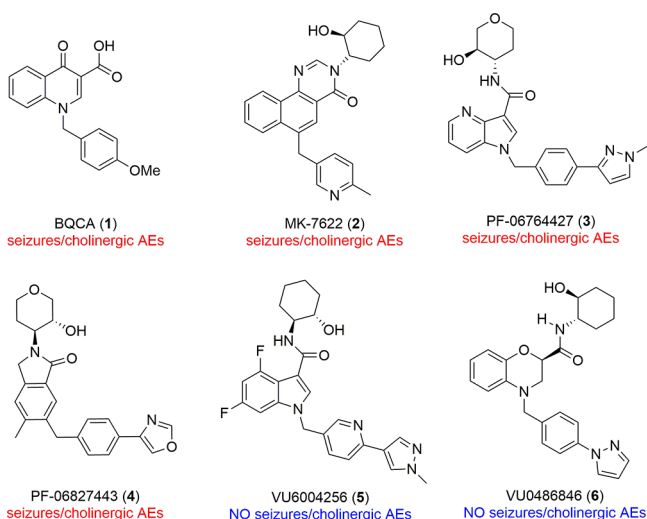


**Figure 1.** Structures of representative  $M_1$  PAMs 1–6. Of these, 1–4 are robust ago-PAMs in high expressing cell lines and native systems, resulting in severe seizures/cholinergic AEs due to overstimulation of  $M_1$ .  $M_1$  PAMs 5 and 6 are devoid of seizures/cholinergic AEs and show little to no  $M_1$  agonism in high expressing cell lines and native systems.

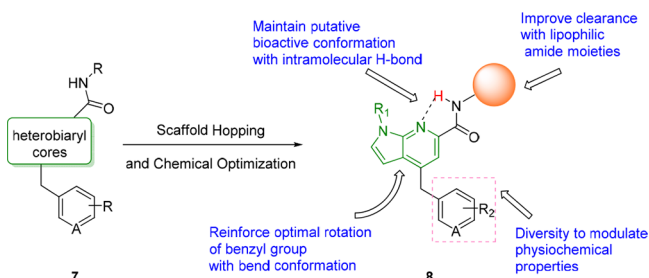
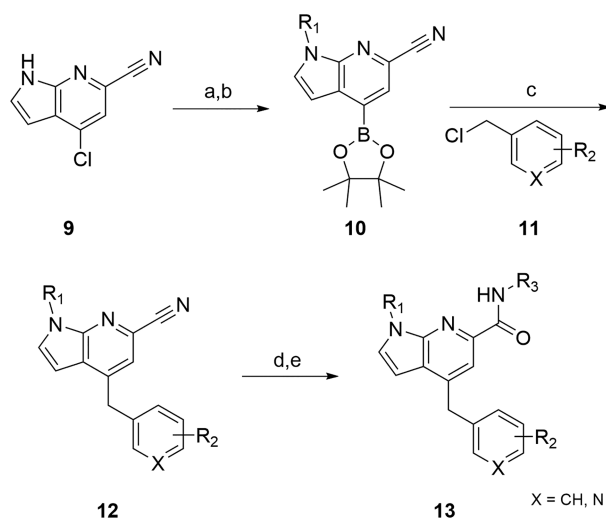


**Figure 2.** Scaffold hopping approach based on  $M_1$  PAMs 3, 5, and 6, which led to the discovery of a novel pyrrolo[2,3-*b*]pyridine carboxamide-based series of  $M_1$  ago-PAMs and pure PAMs, 8.

### Scheme 1. Synthesis of $M_1$ PAM Analogs 13<sup>a</sup>



<sup>a</sup>Reagents and conditions: (a)  $R_1I$ , NaH, DMF, 0 °C–rt, 85–90%; (b) bis(pinacolato)diboron, KOAc, Pd(dppf)Cl<sub>2</sub>, 1,4-dioxane, 100 °C, 16 h, >98%; (c) benzyl chloride, Cs<sub>2</sub>CO<sub>3</sub>, Pd(dppf)Cl<sub>2</sub>, THF/H<sub>2</sub>O, 90 °C, 16 h; 50–84%; (d) conc. HCl, reflux, 2 h, >98%; (e) amine, HATU, DIEA, DMF, rt, 20 min, 35–66%.

hydrolysis of the nitrile and standard HATU amide coupling reactions delivered the putative  $M_1$  PAMs 13 in 35–66% yield.<sup>20</sup>

We then surveyed this new core with a variety of heterobiaryl tails and amide congeners, grouped based on internal knowledge regarding SAR to engender robust  $M_1$  ago-PAM versus PAM activity. The first amide moiety surveyed was the (3*S*,4*R*)-3-hydroxy-4 amino tetrahydropyranyl (THP) amide, well documented to engender potent  $M_1$  PAMs, but with undesired potent  $M_1$  agonist activity.<sup>11,13–17,19</sup> As we previously reported,  $M_1$  PAM potencies below 100 nM, coupled with  $M_1$  agonist activity, generally lead to robust cholinergic AEs.<sup>19</sup> As anticipated, analogs 14 (Table 1) with diverse southern

**Table 1.** Structures and  $M_1$  Pharmacology for Analogs 14<sup>a</sup>

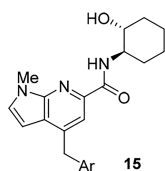
Cpd	R	rM <sub>1</sub> PAM EC <sub>50</sub> (μM) <sup>a</sup> [±SEM]	rM <sub>1</sub> pEC <sub>50</sub> (±SEM)	rM <sub>1</sub> agonist EC <sub>50</sub> (μM) <sup>a</sup> [% ACh Max ±SEM]	rM <sub>1</sub> pEC <sub>50</sub> (±SEM)
14a		0.04 [87±0]	7.41±0.06	2.24 [65±2]	5.65±0.04
14b		0.014 [86±1]	7.86±0.06	0.575 [67±3]	6.24±0.06
14c		0.10 [90±1]	7.00±0.03	5.62 [41±3]	5.25±0.06

<sup>a</sup>Calcium mobilization assays with rat  $M_1$ -CHO cells performed in the presence of an EC<sub>20</sub> fixed concentration of acetylcholine for PAM, and no exogenous ACh for the agonist EC<sub>50</sub>; values represent means from three ( $n = 3$ ) independent experiments performed in triplicate.

heterobiaryl tails provided potent  $M_1$  ago-PAMs. Analog 14b stands out as a 14 nM  $M_1$  PAM (86% ACh max), with an agonist EC<sub>50</sub> of 575 nM (67% ACh max) and a direction not worthy of further pursuit, as overstimulation of  $M_1$  would definitely result.

As the analogous cyclohexyl congener 15 of THP 14 generally afforded a lower degree of  $M_1$  agonism, we next evaluated such analogs. As shown in Table 2, analogs 15 were also potent  $M_1$  ago-PAMs (15a–c), but with reduced  $M_1$  agonism relative to 14,<sup>11,13–17,19</sup> as well as a moderately potent  $M_1$  PAM (15d). Interestingly, both 15b and 15c were not CNS penetrant in rat, with  $K_p$  values below level of quantitation (BLQ), despite favorable CNS MPO scores (4–5).<sup>21</sup> Previously, we have shown that the secondary hydroxyl moiety engenders poor CNS penetration in rodents, and future analogs would avoid this moiety.<sup>19</sup>

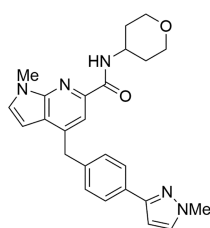
Thus, we evaluated the profile of simple, unsubstituted pyranyl amides, as we hoped this would engender a balance between  $M_1$  PAM potency (and diminished  $M_1$  agonism) and

Table 2. Structures and M<sub>1</sub> Pharmacology for Analogs 15<sup>a</sup>

Cpd	R	rM <sub>1</sub> PAM EC <sub>50</sub> (μM) <sup>a</sup> [% ACh Max ±SEM]	rM <sub>1</sub> pEC <sub>50</sub> (±SEM)	rM <sub>1</sub> agonist EC <sub>50</sub> (μM) <sup>a</sup> [% ACh Max ±SEM]	rM <sub>1</sub> pEC <sub>50</sub> (±SEM)
15a		0.18 [87±1]	6.74±0.03	3.24 [41±2]	5.49±0.02
15b		0.09 [87±1]	7.02±0.04	2.29 [53±2]	5.64±0.04
15c		0.04 [89±1]	7.38±0.04	1.21 [58±3]	5.92±0.05
15d		0.36 [91±1]	6.44±0.01	>30	<4.5

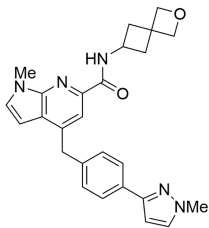
<sup>a</sup>Calcium mobilization assays with rM<sub>1</sub>-CHO cells performed in the presence of an EC<sub>20</sub> fixed concentration of acetylcholine for PAM, and no exogenous ACh for the agonist EC<sub>50</sub>; values represent means from three (*n* = 3) independent experiments performed in triplicate.

CNS penetration. Our initial evaluation produced pyran-2-yl amide **16** and the spiro-cyclic congener **17** (Figure 3); importantly,



16

rM<sub>1</sub> PAM EC<sub>50</sub> = 560 nM, 89% ACh Max  
rM<sub>1</sub> agonist EC<sub>50</sub> >10 μM



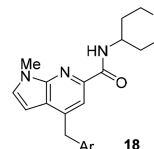
17

rM<sub>1</sub> PAM EC<sub>50</sub> = 604 nM, 91% ACh Max  
rM<sub>1</sub> agonist EC<sub>50</sub> >10 μM

Figure 3. SAR evaluation of nonhydroxylated amides **16** and **17**.

both proved to be pure M<sub>1</sub> PAMs (agonist EC<sub>50</sub>s > 10 μM). However, M<sub>1</sub> PAM potency was modest (**16**: rM<sub>1</sub> PAM EC<sub>50</sub> = 560 nM, pEC<sub>50</sub> = 6.25 ± 0.05, ACh max = 89 ± 1; **17**: rM<sub>1</sub> PAM EC<sub>50</sub> = 604 nM, pEC<sub>50</sub> = 6.22 ± 0.04, ACh max = 91 ± 1). Still, similar pyran-2-yl amides (lacking the secondary hydroxyl moiety) in other series (such as **5** and **6**) were inactive or weak, suggesting this is a unique core. To further optimize M<sub>1</sub> PAM potency with the pyran-2-yl amide, we next explored alternative heterobiaryl tails.

Surprisingly, while holding the pyran-2-yl amide moiety constant in analogs **18** and varying the heterobiaryl tail (Table 3), the lack

Table 3. Structures and M<sub>1</sub> Pharmacology for Analogs 18<sup>a</sup>

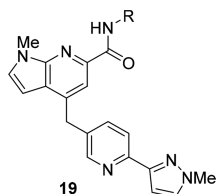
Cpd	R	rM <sub>1</sub> PAM EC <sub>50</sub> (μM) <sup>a</sup> [% ACh Max ±SEM]	rM <sub>1</sub> pEC <sub>50</sub> (±SEM)	rM <sub>1</sub> agonist EC <sub>50</sub> (μM) <sup>a</sup> [% ACh Max ±SEM]	rM <sub>1</sub> pEC <sub>50</sub> (±SEM)
18a		0.49 [87±1]	6.31±0.03	>10 [26±5]	<5
18b		0.76 [90±4]	6.12±0.05	>10 [34±16]	<5
18c		0.23 [93±0]	6.64±0.07	>10	<5
18d		1.74 [78±1]	5.76±0.02	>30	<4.5
18e		0.76 [86±2]	6.12±0.01	>30	<4.5
18f		0.76 [88±3]	6.12±0.03	>10	<5

<sup>a</sup>Calcium mobilization assays with rM<sub>1</sub>-CHO cells performed in the presence of an EC<sub>20</sub> fixed concentration of acetylcholine for PAM, and no exogenous ACh for the agonist EC<sub>50</sub>; values represent means from three (*n* = 3) independent experiments performed in triplicate.

of M<sub>1</sub> agonism in these des-hydroxy congeners proved to be a generally conserved pharmacological property. Of these, **18c** emerged as an attractive M<sub>1</sub> PAM (EC<sub>50</sub> = 230 nM, 93% ACh max; log K<sub>b</sub> = -4.82; log αβ = 2.6) with minimal to no agonism in our high expressing cell line (M<sub>1</sub> agonist EC<sub>50</sub> > 10 μM).<sup>20</sup> Replacement of the *N*-Me pyrazole in **16** for an oxazole analog (e.g., **18f**) provided an M<sub>1</sub> PAM of comparable potency (EC<sub>50</sub> = 760 nM, 88% ACh max) to **16** and still devoid of M<sub>1</sub> agonism. Regioisomeric pyridyl pyrazole heterobiaryls **18b** and **18c** showed similar M<sub>1</sub> PAM activity, but **18b** displayed weak M<sub>1</sub> agonism (~34% @ 10 μM). An *N*-linked pyrazole congener, **18a**, displayed similar PAM potency and weak M<sub>1</sub> agonism (~26% at 10 μM) as well, highlighting the sensitivity of this series for M<sub>1</sub> agonist activity.

A larger amide scan of the pyrazole regioisomers **19** based on the **18b** heterobiaryl tail motif (Table 4) similarly identified a

Table 4. Structures and M<sub>1</sub> Pharmacology for Analogs **19**<sup>a</sup>



Cpd	R	rM <sub>1</sub> PAM EC <sub>50</sub> (μM) <sup>a</sup> [% ACh Max ± SEM]	rM <sub>1</sub> pEC <sub>50</sub> (±SEM)	rM <sub>1</sub> agonist EC <sub>50</sub> (μM) <sup>a</sup> [% ACh Max ± SEM]	rM <sub>1</sub> pEC <sub>50</sub> (±SEM)
<b>15b</b>		0.10 [87±1]	7.02±0.04	2.29 [53±2]	5.64±0.02
<b>19a</b>		0.26 [86±1]	6.59±0.04	>10	<5
<b>19b</b>		0.49 [84±2]	6.31±0.07	>10	<5
<b>19c</b>		1.58 [87±1]	5.80±0.04	>30	<4.5
<b>19d</b>		0.57 [89±1]	6.24±0.06	>30	<4.5
<b>19e</b>		0.55 [94±1]	6.26±0.05	>10	<5

<sup>a</sup>Calcium mobilization assays with rM<sub>1</sub>-CHO cells performed in the presence of an EC<sub>20</sub> fixed concentration of acetylcholine for PAM, and no exogenous ACh for the agonist EC<sub>50</sub>; values represent means from three (*n* = 3) independent experiments performed in triplicate.

number of pure M<sub>1</sub> PAMs and ago-PAMs (with novel amides), but none showed advantages over analogs highlighted in Tables 1–3. However, unlike predecessor series 1–4, this scaffold afforded pure M<sub>1</sub> PAMs, devoid of agonist activity in high expressing M<sub>1</sub> cell lines.

Prior to assessing physicochemical and DMPK properties, we wanted to ensure good species alignment for key M<sub>1</sub> PAMs at both human and rat M<sub>1</sub>. Gratifyingly, there was high species conservation (Table 5), indicating translational potential for this novel series of M<sub>1</sub> PAMs.

The M<sub>1</sub> PAMs highlighted in Table 5 displayed favorable physicochemical properties (MWs < 450, cLogPs between 1.2 and 4.0, TPSAs 89–102 Å<sup>2</sup>, CNS MPO scores between 3.2 and

Table 5. Human and Rat M<sub>1</sub> PAM Activities for Select Analogs 14–18

Cpd	rat M <sub>1</sub> PAM EC <sub>50</sub> (μM) <sup>a</sup> [% ach Max ± SEM]	rat M <sub>1</sub> pEC <sub>50</sub> (±SEM)	hum M <sub>1</sub> PAM EC <sub>50</sub> (μM) <sup>a</sup> [% ACh max ± SEM]	hum M <sub>1</sub> pEC <sub>50</sub> (±SEM)
<b>14a</b>	0.04, [87 ± 0]	7.41 ± 0.06	0.06, [83 ± 3]	7.22 ± 0.10
<b>14c</b>	0.10, [90 ± 1]	7.00 ± 0.03	0.09, [80 ± 8]	7.05 ± 0.20
<b>15a</b>	0.18, [87 ± 1]	6.74 ± 0.03	0.18, [84 ± 2]	6.74 ± 0.10
<b>15b</b>	0.10, [87 ± 1]	7.02 ± 0.04	0.12, [79 ± 4]	6.91 ± 0.10
<b>16</b>	0.56, [89 ± 1]	6.25 ± 0.05	0.66, [87 ± 3]	6.18 ± 0.10
<b>18c</b>	0.23, [93 ± 0]	6.64 ± 0.07	0.32, [84 ± 7]	6.49 ± 0.05

<sup>a</sup>Calcium mobilization assays with rM<sub>1</sub>-CHO or hM<sub>1</sub>-CHO cells performed in the presence of an EC<sub>20</sub> fixed concentration of acetylcholine for PAM; values represent means from three (*n* = 3) independent experiments performed in triplicate.

4.3) and acceptable *in vitro* DMPK profiles (Table 6).<sup>20</sup> The majority show modest predicted hepatic clearance in human and

Table 6. *In Vitro* DMPK Data and PBL Data for Select M<sub>1</sub> PAMs 14–18<sup>a</sup>

property	14a	14c	15b	15c	16	18c
MW	445	446	443	444	427	430
cLogP	2.40	1.22	4.02	2.84	5.21	1.77
TPSA	89.7	102.1	80.5	92.9	60.3	81.9
<i>In Vitro</i> PK Parameters						
rat CL <sub>HEP</sub> (mL/min/kg)	39.1	42.0	49.6	27.3	47.9	44.2
human CL <sub>HEP</sub> (mL/min/kg)	6.97	10.6	17.8	9.3	10.7	6.78
rat <i>f</i> <sub>u</sub> (plasma)	0.03	0.02	0.03	0.06	0.04	0.06
human <i>f</i> <sub>u</sub> (plasma)	0.02	0.02	0.12	0.04	0.02	0.04
rat <i>f</i> <sub>u</sub> (brain)	0.01	0.01	0.04	0.07	0.01	0.08
Rat PBL (IV, 0.2 mg/kg)						
K <sub>p</sub>	0.11	0.21	BLQ	BLQ	BLQ	0.28
K <sub>p,uu</sub>	0.05	0.13	BLQ	BLQ	BLQ	0.32
Mouse PBL (IP, 100 mg/kg)						
K <sub>p</sub>	0.09	ND	0.28	0.03	ND	0.16
K <sub>p,uu</sub>	0.04	ND	0.17	0.04	ND	0.18

<sup>a</sup>BLQ: brain concentration is below limit of quantitation (BLQ) in low dose rat cassette (0.2 mg/kg). ND = not determined.

rat, good free fraction (human, rat, and rat brain homogenate binding), but low to modest CNS penetration in rat (rat brain/plasma K<sub>p</sub>s and K<sub>p,uu</sub>s ≤ 0.3). Moreover, as we have seen significant variations between brain penetration in mice and rats, we also assessed mouse K<sub>p</sub> at 100 mg/kg ip. Despite low but measurable K<sub>p</sub> in mice, brain levels were high (both total and unbound). The low K<sub>p</sub>s were driven by very high plasma concentrations (Supplemental Figure 1).<sup>20</sup>

As we have documented previously,<sup>11,13–17,19</sup> robust ago-PAM activity can lead to over stimulation of the M<sub>1</sub> receptor and/or induce M<sub>1</sub> agonist-dependent long-term depression in the prefrontal cortex leading to cognitive dysfunction and, in mice (the most susceptible species to excessive M<sub>1</sub> activation), Racine scale 4 to 5 seizures.<sup>11,14,17,19</sup> Thus, a quick phenotypic screen in mice (at 100 mg/kg IP) to assess seizure liability has become a proven method of choice to eliminate compounds from the lead progression flow-chart and deem them non-developable. Interestingly, this pyrrolo[2,3-*b*]pyridine carboxamide-based series showed a pronounced tendency for cholinergic adverse effect liability in the mouse seizure model

(Figure 4), with all analogs showing robust Racine scale seizures within 30 min of IP administration (100 mg/kg), save 18c

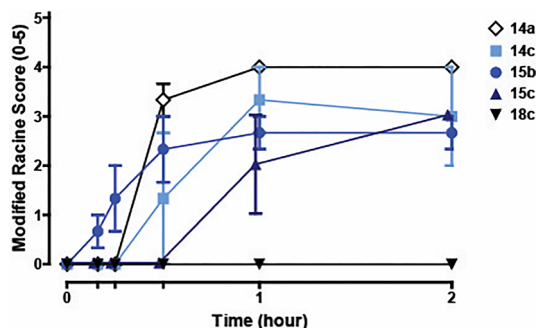


**Figure 4.** Phenotypic mouse seizure assay with compounds dosed at 100 mg/kg i.p. VU6007477 (18c) was devoid of seizure liability (mouse brain levels: 7  $\mu$ M total, 546 nM unbound), whereas 14a, 14c, 15b, and 15c elicited robust Racine scale 4/5 seizures.<sup>20</sup>

(VU6007477). These data further highlight the range of clean versus adverse event (AE) *in vivo* pharmacology that can occur within a highly conserved chemical series of M<sub>1</sub> PAMs (and the value of an informative phenotypic triage screen).<sup>14,19</sup>

Due to the significant AE liability within this series, we were hesitant to further advance this series down the lead optimization flow-chart; however, additional characterization quickly led to a no-go decision for both 18c and this series. While 18c was highly selective for M<sub>1</sub> (M<sub>2</sub>–M<sub>5</sub> EC<sub>50</sub>s > 30  $\mu$ M, Supplemental Figure 2),<sup>20</sup> it proved to be a human P-gp substrate (ER = 4.5), with only moderate permeability (P<sub>app</sub> = 1.2  $\times 10^{-5}$  cm/s). Thus, 18c is a new *in vitro/in vivo* rodent M<sub>1</sub> “pure” PAM tool compound but is not suitable for translation to the clinic.

In summary, a scaffold-hopping exercise identified a novel pyrrolo[2,3-*b*]pyridine carboxamide-based series of M<sub>1</sub> PAMs that displayed a range of potent ago-PAM and pure PAM pharmacology. While congeners possessing the prototypical (3*S*,4*R*)-3-hydroxy-4 amino tetrahydropyranil (THP) amide moiety (or the cyclohexyl analog) engendered a range of M<sub>1</sub> ago-PAM activity, they also resulted in severe Racine scale 4/5 seizures that correlated with the presence of M<sub>1</sub> agonist activity (which is predicted to result in overstimulation of M<sub>1</sub>). In contrast, a simple pyranil amide derivative, 18c (VU6007477), was a pure M<sub>1</sub> PAM in high expressing cell lines (M<sub>1</sub> agonist EC<sub>50</sub> > 10  $\mu$ M), displayed improved CNS penetration over the hydroxylated congeners, and was devoid of seizure liability in mice. While 18c was not advanceable as a clinical candidate, it remains an important new rodent tool compound to study selective M<sub>1</sub> activation without concern for cholinergic toxicity and related AEs. The optimization of other pure M<sub>1</sub> PAMs, devoid of cholinergic toxicity and adverse effect liability, with translational potential, will be reported in due course.

## ■ ASSOCIATED CONTENT

### Supporting Information

The Supporting Information is available free of charge on the ACS Publications website at DOI: 10.1021/acsmchemlett.8b00261.

General methods for the synthesis and characterization of all compounds, and methods for the *in vitro* and *in vivo* DMPK protocols and supplemental figures (PDF)

## ■ AUTHOR INFORMATION

### Corresponding Author

\*Phone: 1 615-322-8700. Fax: 1 615-936-4381. E-mail: craig.lindsley@vanderbilt.edu.

### ORCID

Craig W. Lindsley: 0000-0003-0168-1445

### Author Contributions

C.W.L., C.M.N., P.J.C., H.P.C., and J.M.R. drafted/corrected the manuscript. J.L.E., E.S.C., M.F.L., R.A.C., and D.W.E. performed the chemical synthesis. C.W.L., P.J.C., C.M.N., J.K.R., and H.P.C. oversaw the medicinal chemistry and target selection and interpreted the biological data. V.B.L. and H.P.C. performed the *in vitro* molecular pharmacology studies. A.L.B. performed the *in vitro* and *in vivo* DMPK studies. J.M.R. oversaw the *in vivo* experiments. J.W.D. performed the *in vivo* studies. All authors have given approval to the final version of the manuscript.

### Notes

The authors declare the following competing financial interest(s): Hold IP on M1 PAMs.

## ■ ACKNOWLEDGMENTS

The authors would also like to thank William K. Warren, Jr. and the William K. Warren Foundation who funded the William K. Warren, Jr. Chair in Medicine (to C.W.L.). Studies were supported by the NIH (NIMH, MH082867 and MH108498).

## ■ ABBREVIATIONS

PAM, positive allosteric modulator; PBL, plasma/brain level; AE, adverse event; dppf, 1'-ferrocenediyl-bis-(diphenylphosphine); HATU, 1-[Bis(dimethylamino)methylene]-1*H*-1,2,3-triazolo[4,5-*b*]pyridinium 3-oxid hexafluorophosphate; DIEA, diisopropylethyl amine; DMPK, drug metabolism and pharmacokinetics; MPO, multiparameter optimization

## ■ REFERENCES

- Melancon, B. J.; Tarr, J. C.; Panarese, J. D.; Wood, M. R.; Lindsley, C. W. Allosteric modulation of the M<sub>1</sub> muscarinic acetylcholine receptor: improving cognition and a potential treatment for schizophrenia and Alzheimer's disease. *Drug Discovery Today* **2013**, *18*, 1185–1199.
- Bridges, T. M.; LeBois, E. P.; Hopkins, C. R.; Wood, M. R.; Jones, J. K.; Conn, P. J.; Lindsley, C. W. Antipsychotic potential of muscarinic allosteric modulation'. *Drug News Perspect.* **2010**, *23*, 229–240.
- Levey, A. I.; Edmunds, S. M.; Koliatsos, V.; Wiley, R. G.; Heilman, C. J. Expression of M1-M4 muscarinic acetylcholine receptor proteins in rat hippocampus and regulation by cholinergic innervations. *J. Neurosci.* **1995**, *15*, 4077–4092.
- Levey, A. I. Muscarinic acetylcholine receptor expression in memory circuits: implications for treatment of Alzheimer disease. *Proc. Natl. Acad. Sci. U. S. A.* **1996**, *93*, 13541–13546.
- Felder, C. C.; Porter, A. C.; Skillman, T. L.; Zhang, L.; Bymaster, F. P.; Nathanson, N. M.; Hamilton, S. E.; Gomez, J.; Wess, J.; McKinzie, D. L. Elucidating the role of muscarinic receptors in psychosis. *Life Sci.* **2001**, *68*, 2605–2613.
- Caccamo, A.; Oddo, S.; Billings, L. M.; Green, K. N.; Martinez-Coria, H.; Fisher, A.; LaFerla, F. M. M1 receptors play a central role in modulating AD-like pathology in transgenic mice. *Neuron* **2006**, *49*, 671–682.
- Conn, P. J.; Lindsley, C. W.; Meiler, J.; Niswender, C. M. Opportunities and challenges in the discovery of allosteric modulators of GPCRs for the treatment of CNS disorders. *Nat. Rev. Drug Discovery* **2014**, *13*, 692–708.

(8) Bender, A. M.; Jones, C. K.; Lindsley, C. W. Classics in Chemical Neuroscience: Xanomeline. *ACS Chem. Neurosci.* **2017**, *8*, 435–443.

(9) Ma, L.; Seager, M.; Wittman, M.; Bickel, N.; Burno, M.; Jones, K.; Graufelds, V. K.; Xu, G.; Pearson, M.; McCampbell, A.; Gaspar, R.; Shughrue, P.; Danzinger, A.; Regan, C.; Garson, S.; Doran, S.; Kreatsoulas, C.; Veng, L.; Lindsley, C. W.; Shipe, W.; Kuduk, S.; Jacobson, M.; Sur, C.; Kinney, G.; Seabrook, G. R.; Ray, W. J. Selective activation of the M<sub>1</sub> muscarinic acetylcholine receptor achieved by allosteric potentiation. *Proc. Natl. Acad. Sci. U. S. A.* **2009**, *106*, 15950–15955.

(10) Shirey, J. K.; Brady, A. E.; Jones, P. J.; Davis, A. A.; Bridges, T. M.; Jadhav, S. B.; Menon, U.; Christain, E. P.; Doherty, J. J.; Quirk, M. C.; Snyder, D. H.; Levey, A. I.; Watson, M. L.; Nicolle, M. M.; Lindsley, C. W.; Conn, P. J. A selective allosteric potentiator of the M<sub>1</sub> muscarinic acetylcholine receptor increases activity of medial prefrontal cortical neurons and can restore impairments of reversal learning. *J. Neurosci.* **2009**, *29*, 14271–14286.

(11) Moran, S. P.; Dickerson, J. W.; Plumley, H. C.; Xiang, Z.; Maksymetz, J.; Remke, D. H.; Doyle, C. A.; Niswender, C. M.; Engers, D. W.; Lindsley, C. W.; Rook, J. M.; Conn, P. J. M<sub>1</sub> positive allosteric modulators lacking agonist activity provide the optimal profile for enhancing cognition. *Neuropsychopharmacology* **2018**, *43*, 1763.

(12) Ghoshal, A.; Rook, J.; Dickerson, J.; Roop, G.; Morrison, R.; Jalan-Sakrikar, N.; Lamsal, A.; Noetzel, M.; Poslunsey, M.; Stauffer, S. R.; Xiang, Z.; Daniels, J. S.; Niswender, C. M.; Jones, C. K.; Lindsley, C. W.; Conn, P. J. Selective potentiation of M<sub>1</sub> muscarinic receptors reverses deficits in plasticity and negative and cognitive symptoms in repeated phencyclidine treated mouse model of schizophrenia. *Neuropsychopharmacology* **2016**, *41*, 598–610.

(13) Grannan, M. D.; Mielnik, C. A.; Moran, S. P.; Gould, R. W.; Ball, J.; Bubser, M.; Ramsey, A. J.; Abe, M.; Cho, H. P.; Nance, K. D.; Blobaum, A. L.; Niswender, C. M.; Conn, P. J.; Lindsley, C. W.; Jones, C. K. Prefrontal cortex-mediated impairments in a genetic model of NMDA receptor hypofunction are reversed by the novel M<sub>1</sub> PAM VU6004256. *ACS Chem. Neurosci.* **2016**, *7*, 1706–1716.

(14) Rook, J. M.; Abe, M.; Cho, H. P.; Nance, K. D.; Luscombe, V. B.; Adams, J. J.; Dickerson, J. W.; Remke, D. H.; Garcia-Barrantes, P. M.; Engers, D. W.; Engers, J. L.; Chang, S.; Foster, J. J.; Blobaum, A. L.; Niswender, C. M.; Jones, C. K.; Conn, P. J.; Lindsley, C. W. Diverse effects on M<sub>1</sub> signaling and adverse effect liability within a series of M<sub>1</sub> Ago-PAMs. *ACS Chem. Neurosci.* **2017**, *8*, 866–883.

(15) Davoren, J. E.; O'Neil, S. V.; Anderson, D. P.; Brodney, M. A.; Chenard, L.; Dlugolenski, K.; Edgerton, J. R.; Green, M.; Garnsey, M.; Grimwood, S.; Harris, A. R.; Kauffman, G. W.; LaChapelle, E.; Lazzaro, J. T.; Lee, C.-W.; Lotarski, S. M.; Nason, D. M.; Obach, R. S.; Reinhart, V.; Salomon-Ferrer, R.; Steyn, S. J.; Webb, D.; Yan, J.; Zhang, L. Design and optimization of selective azaindole amides M<sub>1</sub> positive allosteric modulators. *Bioorg. Med. Chem. Lett.* **2016**, *26*, 650–655.

(16) Davoren, J. E.; Lee, C.-W.; Garnsey, M.; Brodney, M. A.; Cordes, J.; Dlugolenski, K.; Edgerton, J. R.; Harris, A. R.; Helal, C. J.; Jenkinson, S.; Kauffman, G. W.; Kenakin, T. P.; Lazzaro, J. T.; Lotarski, S. M.; Mao, Y.; Nason, D. M.; Northcott, C.; Nottebaum, L.; O'Neil, S. V.; Pettersen, B.; Popiolek, M.; Reinhart, V.; Salomon-Ferrer, R.; Steyn, S. J.; Webb, D.; Zhang, L.; Grimwood, S. Discovery of the potent and selective M<sub>1</sub> PAM-agonist *N*-[(3*R*,4*S*)-3-hydroxytetrahydro-2*H*-pyran-4-yl]-5-methyl-4-[4-(1,3-thiazol-4-yl)benzyl]pyridine-2-carboxamide (PF-06767832): Evaluation of efficacy and cholinergic side effects. *J. Med. Chem.* **2016**, *59*, 6313–6328.

(17) Moran, S. P.; Cho, H. P.; Maksymetz, J.; Remke, D.; Hanson, R.; Niswender, C. M.; Lindsley, C. W.; Rook, J. M.; Conn, P. J. PF-06827443 displays robust allosteric agonist and positive allosteric modulator activity in high receptor reserve and native systems. *ACS Chem. Neurosci.* **2018**, DOI: [10.1021/acscchemneuro.8b00106](https://doi.org/10.1021/acscchemneuro.8b00106).

(18) Lange, H. S.; Cannon, C. E.; Drott, J. T.; Kuduk, S. D.; Uslaner, J. M. The M<sub>1</sub> muscarinic positive allosteric modulator PQCA improves performance on translatable tests of memory and attention in rhesus monkeys. *J. Pharmacol. Exp. Ther.* **2015**, *355*, 442–450.

(19) Rook, J. M.; Berton, J. L.; Cho, H. P.; Gracia-Barrantes, P. M.; Moran, S. P.; Maksymetz, J. T.; Nance, K. D.; Dickerson, J. W.; Remke,

D. H.; Chang, S.; Harp, J. M.; Blobaum, A. L.; Niswender, C. M.; Jones, C. K.; Stauffer, S. R.; Conn, P. J.; Lindsley, C. W. A novel M<sub>1</sub> PAM VU0486846 exerts efficacy in cognition models without displaying agonist activity or cholinergic toxicity. *ACS Chem. Neurosci.* **2018**, DOI: [10.1021/acscchemneuro.8b00131](https://doi.org/10.1021/acscchemneuro.8b00131).

(20) See [Supporting Information](#) for full details.

(21) Wager, T. T.; Hou, X.; Verhoest, P. R.; Villalobos, A. Central nervous system multiparameter optimization desirability: application in drug discovery. *ACS Chem. Neurosci.* **2016**, *7*, 767–775.